Trapping of kinks and solitons by defects: Phase space transport in finite dimensional models*

Philip J. Holmes† Roy H. Goodman‡ Michael I. Weinstein§

August 27, 2001

Abstract

We study models of Fei et. al. [1] and Forinash et. al. [2] of kinks in the sine-Gordon equation, and solitons in the nonlinear Schrödinger equation interacting with point defects. The models are two and three degree-of-freedom Hamiltonian systems. Using dynamical systems methods, we show that they exhibit interesting behaviors including transverse heteroclinic orbits to degenerate equilibria at infinity, chaotic dynamics, and complex and delicate structures describing the interaction of travelling waves with the defect. We interpret the behavior in terms of invariant manifolds and phase space transport theory.

1 Introduction and motivation

In this paper we summarise current work on the interaction of traveling waves with defects in media (local variations in material properties or geometry); detailed accounts appear in [3, 4]. Motivated by a desire to understand light-trapping by specially engineered defects in optical fiber waveguides [5], we study two simpler problems: kink-impurity interations in the sine-Gordon equation, and soliton-impurity interactions in the nonlinear Schrödinger equation. In both cases we take ordinary differential equation (ODE) models formally derived from the governing partial differential equations (PDE) by substitution of a two-mode *ansatz* having fixed spatial forms and time-dependent amplitude and phase coefficients. Employing the Lagrangian (variational) formulation,

*Invited paper at the Conference on Progress in Nonlinear Science, in honor of the 100th anniversary of the birth of Alexander A. Andronov, held at the University of Nizhny Novgorod, Russia, July 2-6th, 2001.

†Program in Applied and Computational Mathematics and Department of Mechanical and Aerospace Engineering, Princeton University, Princeton, NJ 08544

‡Mathematical Sciences Research, Bell Laboratories–Lucent Technologies, Murray Hill, NJ 07974 and Program in Applied and Computational Mathematics, Princeton University, Princeton, NJ

§Mathematical Sciences Research, Bell Laboratories–Lucent Technologies, Murray Hill, NJ 07974

and taking variations only in the finite-dimensional subspace spanned by these modes, Fei et. al. [1] and Forinash et. al. [2] derived ODEs, studied them numerically and semi-analytically, and compared those results with direct simulations of the PDEs. We carry out a more detailed study of the ODEs in their Hamiltonian formulations, and show that certain aspects of the interaction between the travelling wave and standing 'impurity' mode can be understood in terms of coupled mode interations interpreted geometrically in state space.

This paper is organized as follows. In Section 2 we review the two-mode model of Fei, Kivshar, and Vázquez [1], develop a Hamiltonian formulation with a coupling parameter, and describe a Melnikov-type analysis that establishes transverse homoclinic orbits to certain periodic orbits 'at infinity' corresponding to the non-interacting modes. This in turn permits the phase-space transport analysis of Section 3 that illuminates the dynamics of transmission, reflection, and (transient) trapping of kinks. Section 4 describes a modified three-mode version of the model of Forinash et. al. [2]. Using a cyclic coordinate and the corresponding conserved momentum, we again obtain a two degree-of-freedom model. While this also exhibits transverse homoclinic orbits to infinity, we focus on a different transmission-reflection mechanism, involving stable and unstable manifolds of a set of periodic orbits on an invariant plane corresponding to the standing impurity mode alone. We summarize in Section 5.

Since this paper ultimately concerns nonlinear physics, and employs dynamical system models in the form of coupled oscillators, we believe that it is a suitable tribute to Alexander Alexandrovich Andronov, whose pioneering work in Gorki was so important to the development of dynamical systems, control theory, and nonlinear science in general, eg. [6].

2 An ODE model for kink trapping

Consider the sine-Gordon equation with a localized impurity (point defect) of strength ϵ (not necessarily small) at the origin:

$$u_{tt} - u_{xx} + \sin u = \epsilon\delta(x)\sin u. \tag{2.1}$$

In the absence of defects ($\epsilon = 0$) (2.1) supports a family of kink solutions parameterized by speed V:

$$u_k(x,t) = 4\tan^{-1}\exp\left((x - Vt - x_0)/\sqrt{1-V^2}\right). \tag{2.2}$$

Fei et. al. [1] investigated (2.1) and noted three possible behaviors for kink solutions initialised at large x_0. Above a critical velocity V_c, the kink passes through the defect, emerging with diminished speed, below V_c the kink is captured, except in certain 'resonance bands' where it 'interacts a finite number of times with the defect' before returning in the direction from which it came. Figure 9 of [1] illustrates this behavior.

To derive the ODE model, Fei et. al. [1] substitute the *ansatz*:

$$u = u_k + u_{im} = 4\tan^{-1}\exp\left(x - X(t)\right) + a(t)e^{-\epsilon|x|/2} \tag{2.3}$$

into the Lagrangian of (2.1) and evaluate the spatial integrals to obtain

$$L = \int_{-\infty}^{\infty} \left(\frac{1}{2} u_t^2 - \frac{1}{2} u_x^2 - [1 - \epsilon\delta(x)](1 - \cos u) \right) dx \Rightarrow$$
$$L_{\text{eff}} = 4\dot{X}^2 + \frac{1}{\epsilon}(\dot{a}^2 - \Omega^2 a^2) - U(X) - aF(X). \tag{2.4}$$

The Euler-Lagrange equations for (2.4) yield the coupled oscillator system:

$$8\ddot{X} + U'(X) + aF'(X) = 0, \tag{2.5a}$$
$$\ddot{a} + \Omega^2 a + \frac{\epsilon}{2} F(X) = 0, \tag{2.5b}$$

where U and F are the 'potentials'

$$U(X) = -2\epsilon \operatorname{sech}^2(X) \quad \text{and} \quad F(X) = -2\epsilon \tanh(X) \operatorname{sech}(X). \tag{2.6}$$

Here $X(t)$ denotes the kink location ($X \sim x_0 + Vt$ of (2.2)) and $a(t)$ the amplitude of the impurity mode. Numerical studies of (2.5) reveal behavior similar to that noted by Fei et. al. for the PDE, with the difference that the trapping bands below V_c are replaced by bands in which the orbit is trapped for a finite time before being transmitted past the defect. There is no evidence of trapping for all time. See Figure 3.2 of [3].

We rewrite Equations (2.5) in Hamiltonian form with momentum variables

$$p_X = \frac{\partial L_{\text{eff}}}{\partial \dot{X}} = 8\dot{X}, \qquad p_a = \frac{\partial L_{\text{eff}}}{\partial \dot{X}} = \frac{2}{\epsilon}\dot{a}, \tag{2.7}$$

and define action-angle coordinates for the impurity mode:

$$a = \sqrt{\frac{I\epsilon}{\Omega}} \cos\theta, \qquad p_a = 2\sqrt{\frac{\Omega I}{\epsilon}} \sin\theta, \tag{2.8}$$

so that the Hamiltonian of the full system becomes

$$H(X, p_X, I, \theta) = \frac{1}{16} p_X^2 + U(X) + \Omega I + \mu \sqrt{\frac{I\epsilon}{\Omega}} \cos\theta \, F(X) \stackrel{\text{def}}{=} H^0 + \mu H^1. \tag{2.9}$$

Here we have also introduced an artificial coupling parameter μ (in fact $\mu = 1$) for perturbative analysis. Indeed, when $\mu = 0$ Hamilton's equations decouple (cf. (2.5) with the F term omitted) into a harmonic impurity mode $a = a_0 \cos\Omega(t - t_0)$ and the kink dynamics of Figure 2.1, containing the separatrix Γ formed by a pair of homoclinic orbits to infinity, given by

$$p_X^0 = \pm 4\sqrt{2\epsilon} \operatorname{sech} X^0 \; ; \; X^0 = \pm \sinh^{-1} \sqrt{\frac{\epsilon}{2}} (t - t_1). \tag{2.10}$$

Γ divides the (X, p_X)-phase plane into three invariant regions: R_1 and R_3, filled with orbits passing from $\mp\infty$ to $\pm\infty$, and R_2, containing trapped (periodic) orbits. For $\mu \neq 0$ the kink can interact with the impurity mode and cross between

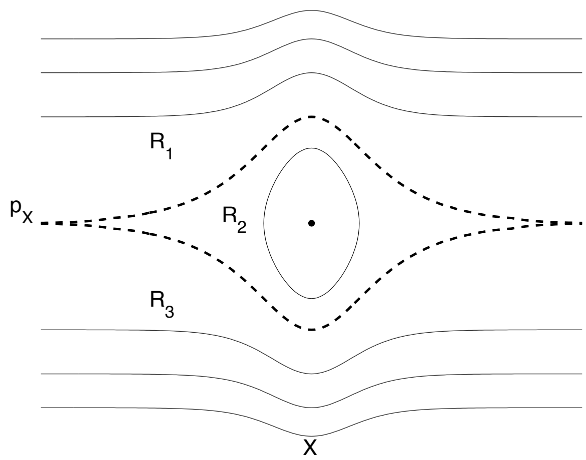

Figure 2.1: The phase plane for the uncoupled X system

R_1 and R_2 or R_2 and R_3: the periodic perturbation due to the oscillatory mode causes the separatrices to split. A kink will be said to be (transiently) trapped or captured if it starts in R_1 or R_3 and then enters and stays in R_2 for (finite) future times.

We first appeal to a theorem of McGehee [7] to prove that the stable and unstable manifolds to the family of degenerate saddle type orbits ($X = \pm\infty, p_X = 0, I = I^0, \theta = \Omega t + \theta_0$) at infinity persist for $\mu \neq 0$. We then use reduction to a constant energy manifold $H^0 + \mu H^1 = h^0$ [8, Section 4.8], thus eliminating I and replacing time by the time-like phase variable θ and recasting the problem as a periodically forced oscillator. As such, we may define a cross section $\Sigma_0 = \{(X, p_X, \theta = \theta_0)\}$ and the associated Poincaré map P_{θ_0}. The Melnikov method [9], cf [8, Theorem 4.8.4], is then used to compute a first order estimate of the splitting distance:

$$\begin{aligned} M(\theta_0) &= \int_{-\infty}^{\infty} \left(\frac{\partial H^X}{\partial X}\frac{\partial H^1}{\partial p_X} - \frac{\partial H^X}{\partial p_X}\frac{\partial H^1}{\partial X} \right) dt \\ &= -\epsilon^2 \sqrt{\frac{2I^0}{\Omega}} \int_{-\infty}^{\infty} \cos(\Omega t + \theta_0)\,\mathrm{sech}^2 X (1 - 2\,\mathrm{sech}^2 X) dt \\ &= 2\pi\sqrt{2I^0}\epsilon \left(1 - \frac{\epsilon^2}{4}\right)^{1/4} e^{-\sqrt{\frac{2}{\epsilon} - \frac{\epsilon}{2}}} \cos\theta_0. \end{aligned} \tag{2.11}$$

Here the integral is evaluated along the unperturbed separatrix (2.10). Since $M(\theta_0)$ has simple zeroes in the admissible range $\epsilon \in (0, 2)$) for each $I^0 > 0$, we conclude that the stable and unstable manifolds of each periodic orbit $I = I^0$ at $X = \pm\infty$ intersect transversally. Figure 2.2 shows a numerical computation of part of the manifolds on the cross section $\Sigma = \{(X, p_X, \theta = \pi/2)\}$.

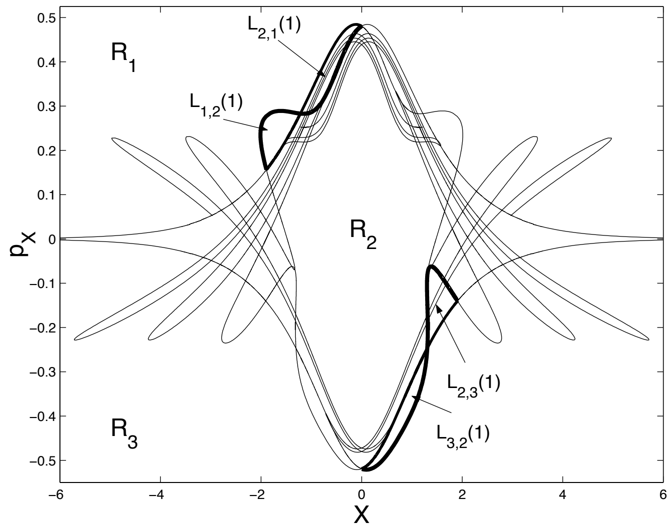

Figure 2.2: The stable and unstable manifolds of the fixed points at $X = \pm\infty$ for the Poincaré map $P_{\pi/2}$, with parameters $\mu = 0.5$, $\epsilon = 0.5$, $I^0 = 0.5$. Turnstile lobe boundaries indicated by bold portions.

This perturbative analysis is for small μ, but in [3] we show by direct esimates on the ODEs (2.5) that homoclinic orbits persist to $\mu = 1$.

3 Phase space transport

The phase space transport theory of Rom-Kedar and Wiggins [10, 11] is applicable to the map P_{θ_0} derived above. Consider a kink starting in region R_1 to the left of and above the (unperturbed) separatrix. If it is to enter R_2 it must lie below the stable manifold of $X = +\infty$: hence, inside one of the *lobes* to the left of $X = 0$ and bounded below by the unstable manifold of $X = -\infty$, eg. $L_{1,2}(1)$ on Figure 2.2. (The lobe $L_{i,j}(k)$ is the set of all points in region R_i which are mapped to region R_j under k iterations of P_{θ_0}: only a finite set of lobes is shown, they march off to $\pm\infty$). Similarly, if an orbit is to escape R_2 to R_1 or R_3, it must do so via $L_{2,1}(1)$ or $L_{2,3}(1)$. These 'one-step' lobes $L_{i,j}(1)$ are called *turnstiles*. Moreover, as Figure 2.2 shows, the iterative structure of homoclinic intersections implies that each turnstile is crossed by preimages of other lobes, so that orbits may be trapped for a finite number of iterates of P_{θ_0} before being ejected once more. In fact, the area-preservation of P_{θ_0} and arguments like those used in proof of the Poincaré Recurrence Theorem lead to:

Proposition 1. *The set of points in $R_1 \cup R_3$ that is captured in R_2 and trapped for all future iterates, is of Lebesgue measure zero.*

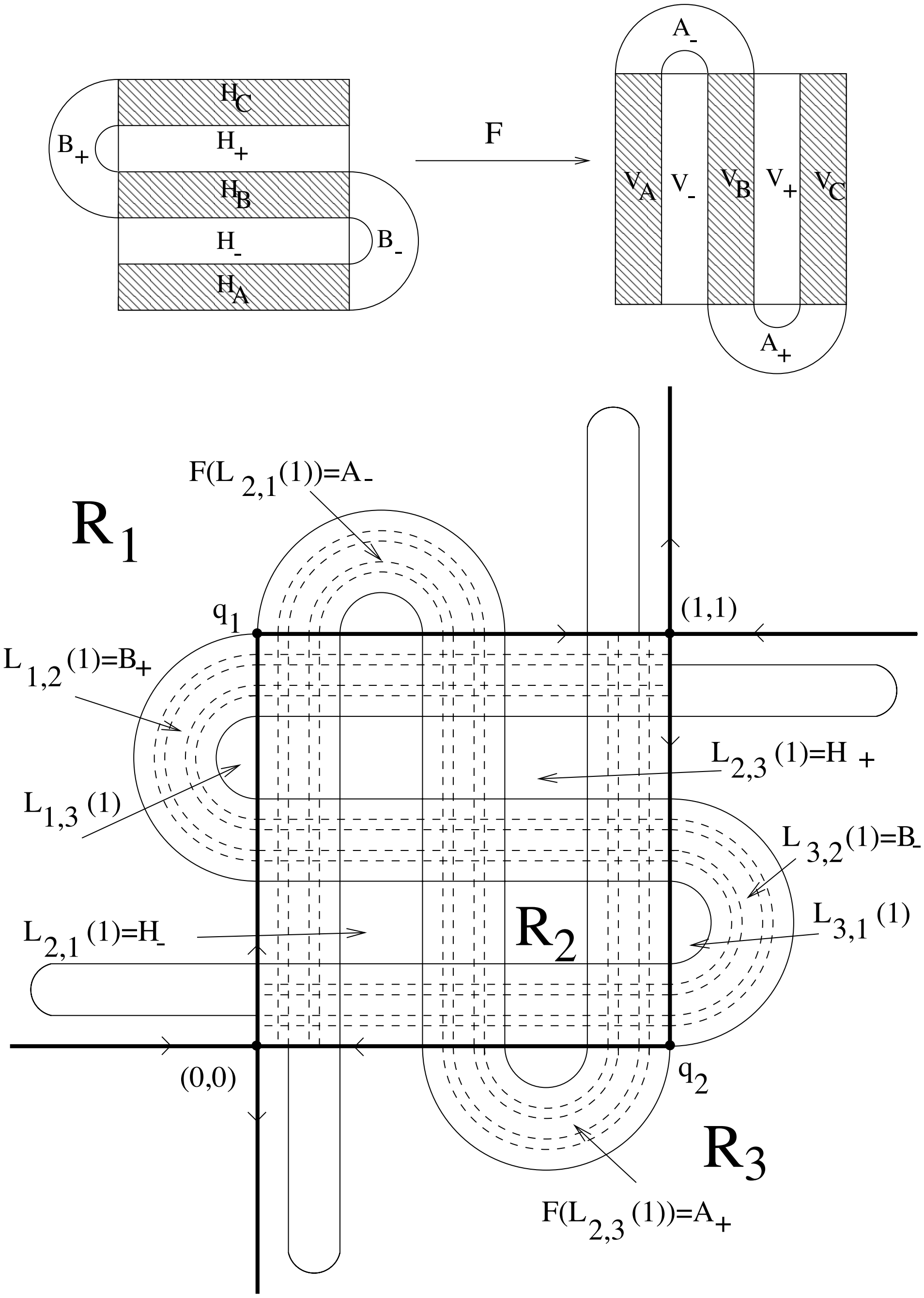

Figure 3.1: A soluble trapping model.

The set of points trapped for all time has the local structure of the product of a Cantor set and an arc, and the gaps of the Cantor set correspond to orbits which are trapped for a finite number of iterates and then ejected. To illustrate this, we consider an explicitly soluble example based on the standard Smale horseshoe [12, 8]. Figure 3.1 shows a map F defined on the unit square $S = [0,1]\times[0,1]$, with three hyperbolic saddle points at $(0,0)$, $(0.5,0.5)$ and $(1,1)$. F is piecewise linear on the three horizontal strips H_i, $i = A, B, C$, whose images are the vertical strips $V_i = F(H_i)$. The definition of F is completed by specifying its nonlinear action on the strips $H_\pm$ and that of F^{-1} on $V_\pm$: see the top of Figure 3.1. The points $(1,1)$ and $(0,0)$ correspond to the degenerate equilibria of P_{θ_0} at $\pm\infty$, and we focus on transport among regions R_1 (upper left), R_3 (lower right) and $R_2 = S$ (the unit square itself). The reader can check that the turnstile lobes $L_{1,2}(1) = B_+$, $L_{2,1}(1) = H_-$, $L_{3,2}(1) = B_-$ and $L_{2,3}(1) = H_+$ are as shown.

A careful analysis [3] of the corresponding turnstiles and lobe-intersections of F, along with its piecewise linearity on H_i, allows us to compute the measure $A(k)$ of sets of points trapped in R_2 for given numbers (k) of iterates. These correspond to gaps in the iterative Cantor set construction apparent in Figure 3.1; the set trapped for all time is the (zero measure) stable manifold of the horseshoe itself. We obtain

$$A(k) = 2\alpha\,(1-2\alpha)^{k-1} = \frac{\lambda_u - 3}{\lambda_u}\left(\frac{3}{\lambda_u}\right)^{k-1}, \tag{3.1}$$

where $\lambda_u > 3$ is the expansion factor (unstable eigenvalue) of $DF|_{H_i}$. Note that $\sum_{k=1}^{\infty} A(k) = 1$: as we expect from Proposition 1, the Cantor set itself is of measure zero. Moreover, plotting $A(k)$ *vs.* k, we obtain the distribution of residence times for trapped orbits as an exponentially decaying curve. We test this prediction for the sine-Gordon model in Figure 3.2, which was obtained by seeding $L_{1,2}(1)$ with 5,000 points, computing their orbits and recording their residence times in R_2. Decay (with an exponent $\approx -.038$) is clear.

The topological transport picture sketched above helps explain the observation of reflection and trapping windows, noted in Section 2, as follows. Orbits starting above the turnstile lobe $L_{1,2}(1)$ and its preimages are transmitted directly; those starting in a preimage of $L_{1,2}(1)$ are trapped, however, as for the piecewise linear model F, trapping is transient, with exponentially decaying probability of remaining within R_2 for time T. Orbits in a preimage of $L_{2,1}(1)$ are eventually transmitted, and those in a preimage of $L_{2,3}(1)$ are eventually reflected. Similar observations apply to orbits starting at $+\infty$ in R_3.

Inclusion of radiation-induced dissipation in the ODEs, due to coupling of the modes $u_k + u_{im}$ with the continuum, supplements (2.5b) with a nonlinear damping term of the form $-\epsilon^3 \Gamma F(X)^2 a^2 \dot{a}$. The flow becomes volume-contracting and the stable manifold of the trivial solution $(X = 0, p_X = 0, I = 0)$ invades the turnstiles and lobes. The result is that the number of reflection and transmission bands becomes finite and windows of data trapped for all time open for speeds $V < V_c$. See [3] Figure 6.1. As Γ increases, transmission bands successively vanish, and the qualitative behavior appears to approach that of the PDE.

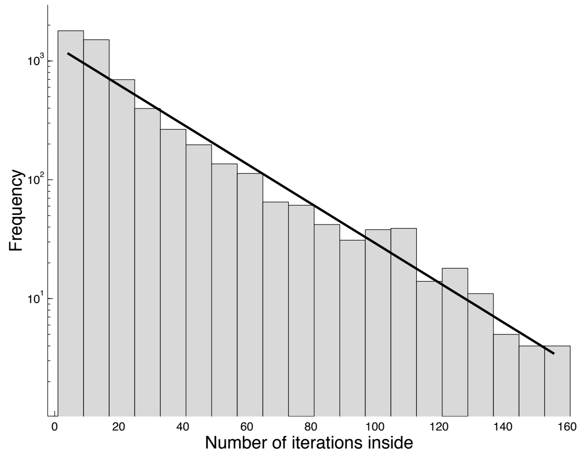

Figure 3.2: A histogram of residence times in R_2.

4 An ODE model for soliton trapping

We consider a nonlinear Schrödinger system with a localized impurity at the origin:

$$iu_t + \frac{1}{2}u_{xx} + |u|^2 u + \gamma\delta(x)u = 0. \tag{4.1}$$

Much as in Section 2, but modifying the *ansatz* of [2], we substitute into (4.1)

$$u = \eta\,\mathrm{sech}(\eta x - Z)e^{i(Vx-\phi)} + a\,\mathrm{sech}\,(a|x| + \tanh^{-1}\frac{\gamma}{a})e^{-i\phi-i\psi} : \tag{4.2}$$

the sum of a 'generalized' soliton and a bound state based on the exact defect mode with frequency-dependent amplitude. Following the same procedure, we obtain a three degree-of-freedom system with Hamiltonian

$$H = -\left(\frac{\eta^3 + a^3}{3}\right) + \eta V^2 - \gamma\eta^2\,\mathrm{sech}^2\,Z - 2\gamma\eta\sqrt{a^2-\gamma^2}\,\mathrm{sech}\,Z\cos\psi, \tag{4.3}$$

in which the variables V, ϕ, and ψ correspond to generalized positions and the generalized momenta are given by

$$p_V = -2Z\ ,\ p_\phi = 2\eta + 2(a-\gamma)\ ,\ p_\psi = 2(a-\gamma). \tag{4.4}$$

Note that, since the angle ϕ is absent from H, its conjugate momentum p_ϕ is also conserved: $(\eta + a - \gamma) = c - \gamma =$ const: this corresponds to L_2-norm $||u||$-conservation in (4.1). Thus the $\dot{\phi}$ equation decouples and the system reduces to two degrees of freedom.

It is convenient to write the resulting equations of motion in terms of the variables (Z, V, a, ψ), with $\eta = c - a$ implicity defined:

$$\dot{Z} = \eta V, \tag{4.5a}$$

$$\dot{V} = -\gamma\eta^2 \operatorname{sech}^2 Z \tanh Z - \gamma\eta\sqrt{a^2-\gamma^2} \operatorname{sech} Z \tanh Z \cos\psi, \tag{4.5b}$$

$$\dot{a} = -\gamma\eta\sqrt{a^2-\gamma^2} \operatorname{sech} Z \sin\psi, \tag{4.5c}$$

$$\dot{\psi} = \frac{1}{2}(\eta^2 - \gamma^2 - V^2) + \gamma\eta \operatorname{sech}^2 Z + \gamma\left(\frac{a^2 - \eta a - \gamma^2}{\sqrt{a^2-\gamma^2}}\right) \operatorname{sech} Z \cos\psi. \tag{4.5d}$$

Note that γ can be scaled out of these equations, so w.l.o.g. we may set $\gamma = 1$ and consider the system (4.5) with parameter $c > \gamma = 1$. Note that at $Z = \pm\infty$ (or $|Z| \gg 1$) the initial data η_0, a_0 and V_0 determine the conserved quantities $H = h_0$ and c. If $\eta = c - \gamma$ all the energy is in the soliton, if $\eta = 0$ $(a = c)$ it is all in the impurity mode; in any case a is confined to the invariant domain $a \in (\gamma, c)$.

While one can apply the same perturbation method to (4.5) as above, few of the interesting phenomena occur in parameter ranges for which $\dot{\psi} > 0$ and the reduction procedure goes through. Here, therefore, we consider a different mechanism that determines the transmission/reflection fate of orbits in the particular case $\eta < \gamma$. Further details and generalisations will appear in [4].

Figure 4.1 shows projections on the (Z, V) plane of two solutions started at $Z_0 = -20, a_0 = \gamma$[1] with fixed $\eta_0 = c - a_0$ and differing velocities V_0: one is transmitted, the other reflected. In fact there is a critical velocity V_c depending on η_0 (or $c = \eta_0 + \gamma$) such that all solitons initialised with $V_0 > V_c$ are transmitted and those with $V_0 < V_c$ are reflected with no (prolonged) interaction.

This behavior may be understood as follows. The 'critical' solutions near $V_0 = V_c$ spend a significant period near the invariant plane $\mathcal{P} = \{Z = V = 0\}$. On that plane the two-dimensional system (4.5c-4.5d), with $Z = V \equiv 0$, is completely integrable and possesses a center at (a^*, π) surrounded by a family of periodic orbits $\mathcal{O}_{h_0}$, parameterised by the value $H = h_0$, limiting on saddle separatrices. In the larger state space the fixed point $(0, 0, a^*, \pi)$ is a saddle-center, with real eigenvalues having eigenvectors lying outside $\mathcal{P}$. Linearising along any periodic orbit $(\bar{a}(t), \bar{\psi}(t))$ enclosing (a^*, π) gives a problem in Floquet theory [13] that block-diagonalises into a piece in $\mathcal{P}$ (with Floquet multipliers 1 and 1) and a piece determining the stability outside $\mathcal{P}$: the Hill's equation

$$\dot{Z} = (c - \bar{a}(t))V, \tag{4.6a}$$

$$\dot{V} = -\gamma\left((c - \bar{a}(t))^2 + (c - \bar{a}(t))\sqrt{\bar{a}(t)^2 - \gamma^2}\cos\bar{\psi}(t)\right) Z. \tag{4.6b}$$

For $\eta < \gamma$ we find (numerically) that the Floquet discriminant is greater than 2 in magnitude, and hence that all these periodic orbits are also hyperbolic transverse to $\mathcal{P}$. Each of these orbits therefore possesses two-dimensional stable and unstable manifolds $W^{s,u}(\mathcal{O}_{h_0})$, and the stable manifolds locally separate the

[1] To avoid the square root singularity, we set $a_0 = \gamma + \varepsilon$, $\varepsilon \ll 1$.

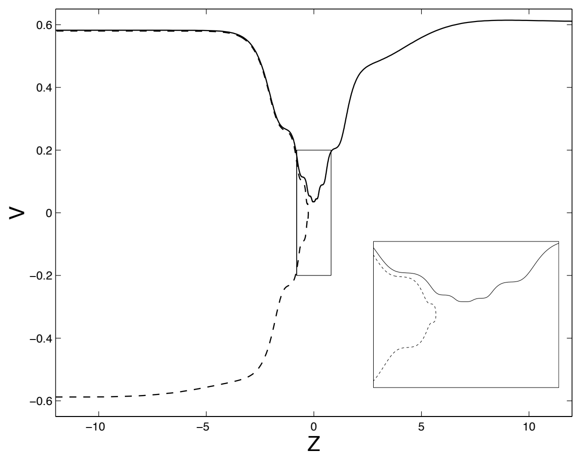

Figure 4.1: Projections of reflected and transmitted NLS solitons on the (Z, V)-plane. Inset shows enlargement of orbits near the origin.

three-dimensional energy manifold $H = h_0$ into components containing orbits that are transmitted and reflected. The union $W^s(\mathcal{P}) = \cup_{h_0} W^s(\mathcal{O}_{h_0})$, a three-dimensional manifold, generically intersects the 'incoming' three-dimensional cross sections $\Sigma_{Z_0} = \{Z = Z_0\}$ in two-dimensional surfaces that separate transmitted and reflected orbits, thereby implicitly defining the the set of critical velocities V_c which are, in turn, further constrained for large $|Z_0|$ by conservation of H:

$$V = \pm\sqrt{\left(\frac{c^3/3 + h_0}{c - a} - c\,a\right)}. \tag{4.7}$$

Figure 4.2 shows projections of the solutions of Figure 4.1 onto $\mathcal{P}$, compared with orbits lying on that plane.

5 Conclusions

In this paper we have reviewed recent and ongoing work in which a two-mode *ansatz* is used to formally reduce perturbed infinite dimensional evolution equations to finite-dimensional ODE models. Specifically, we consider trapping of travelling kink and soliton solutions of the single space dimension sine-Gordon and nonlinear Schrödinger equations with point (delta function) impurities located at the origin. The ODEs recast the problems as modal interactions in two degree-of-freedom Hamiltonian systems.

In the sine-Gordon problem, the key mechanism explaining transmission, reflection, and transient trapping involves transverse intersections of homoclinic orbits to a degenerate periodic orbit 'at infinity,' in which the impurity mode

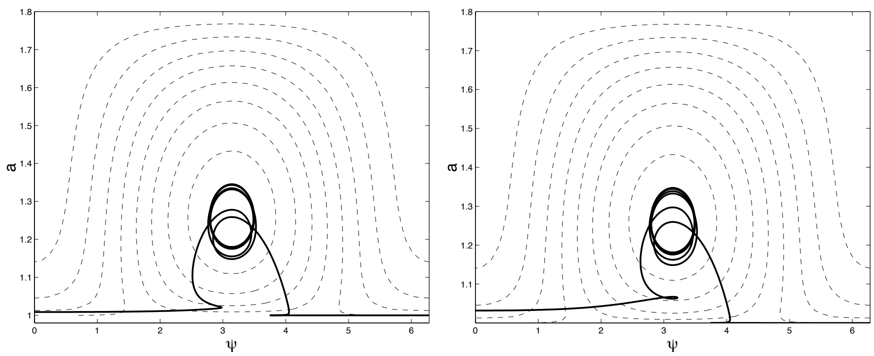

Figure 4.2: Projections of reflected and transmitted NLS solitons compared with the (a, ψ)-flow on the invariant subspace $\mathcal{P}$.

does not interact with the distant kink. Phase space transport methods then permit one to interpret trapping in terms of a Smale horseshoe in a Poincaré map for the reduced flow on a constant energy surface.

In the nonlinear Schrödinger equation, while similar homoclinic orbits and transport phenomena occur for sufficiently large amplitude solitons, a different mechanism governs the simple boundary separating transmission and reflection for low amplitudes. This is the stable manifold of a set of periodic orbits 'at the origin,' in which the impurity mode oscillates uncoupled to the soliton which is stalled over the defect.

We hope that these examples illustrate that the geometrical view of dynamical systems, pioneered by Poincaré and extensively developed by A.A. Andronov and the Gorki school, can illuminate areas considerably beyond their direct application to ODEs.

Acknowledgements: PH was partially supported by DoE: DE-FG02-95ER25238. RG was supported by NSF DMS-9901897 and Bell Laboratories/Lucent Technologies under the Postdoctoral Fellowship with Industry Program.

References

[1] Z. Fei, Y. S. Kivshar, and L. Vázquez. Resonant kink-impurity interactions in the sine-Gordon model. *Phys. Rev. A*, 45:6019–6030, 1992.

[2] K. Forinash, M. Peyrard, and B. Malomed. Interaction of discrete breathers with impurity modes. *Phys. Rev. E*, 49:3400–3411, 1994.

[3] R. H. Goodman, P. J. Holmes, and M. I. Weinstein. Interaction of sine-Gordon kinks with defects: Phase space transport in a two-mode model. *Physica D (in review)*, 2001.

[4] R. H. Goodman, P. J. Holmes, and M. I. Weinstein. Interaction of NLS solitons with defects: Phase space transport in a finite-dimensional model. *in preparation.*

[5] R. H. Goodman, R. E. Slusher, and M. I. Weinstein. Stopping light on a defect. *submitted to J. Opt. Soc. Am. B*, 2001.

[6] A.A. Andronov, E.A. Vitt, and S.E. Khaiken. *Theory of Oscillators.* Pergamon Press, Oxford, U.K., 1966. Reprinted by Dover Publications Inc, NY, 1987.

[7] R. McGehee. A stable manifold theorem for degenerate fixed points with applications to celestial mechanics. *J. Differential Equations*, 14:70–88, 1973.

[8] J. Guckenheimer and P. Holmes. *Nonlinear oscillations, dynamical systems, and bifurcations of vector fields.* Springer-Verlag, New York, 1983.

[9] V. K. Melnikov. On the stability of the center for time periodic perturbations. *Trans. Moscow Math. Soc.*, 12:1, 1963.

[10] V. Rom-Kedar and S. Wiggins. Transport in two-dimensional maps. *Arch. Rational Mech. and Analysis*, 109:239–298, 1990.

[11] S. Wiggins. *Chaotic transport in dynamical systems.* Springer-Verlag, New York, 1992.

[12] S. Smale. Differentiable dynamical systems. *Bull. Amer. Math. Soc.*, 73:747–817, 1967.

[13] P. Hartman. *Ordinary Differential Equations.* Wiley Publishing Co., New York., second, corrected edition, 1964.